Double dynamic hydrogels formed by wormlike surfactant micelles and cross-linked polymer

Andrey V. Shibaev [a], Alexander I. Kuklin [b,c], Vladimir N. Torocheshnikov [d], Anton S. Orekhov [c,e], Sébastien Roland [f], Guillaume Miquelard-Garnier [f], Olga Matsarskaia [g], Ilias Iliopoulos [f], Olga E. Philippova [a,*]

[a] *Physics Department, Lomonosov Moscow State University, Moscow 119991, Russia*
[b] *Frank Laboratory of Neutron Physics, Joint Institute for Nuclear Research, Dubna 141980, Russia*
[c] *Moscow Institute of Physics and Technology, Dolgoprudny 141701, Russia*
[d] *Chemistry Department, Lomonosov Moscow State University, Moscow 119991, Russia*
[e] *A.V. Shubnikov Institute of Crystallography, Moscow 119333, Russia*
[f] *Laboratoire PIMM, Arts et Metiers Institute of Technology, CNRS, Cnam, HESAM Universite, Paris 75013, France*
[g] *Institut Laue-Langevin, Grenoble 38042, France*

GRAPHICAL ABSTRACT

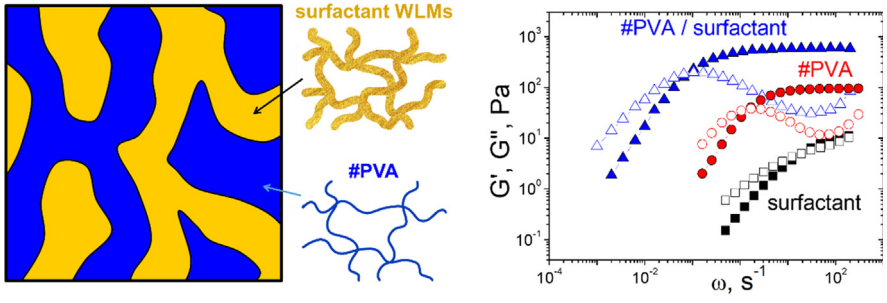

Keywords:
Surfactants
Self-assembly
Wormlike micelles
Hydrogels
Polymer networks

ABSTRACT

Hypothesis: Interpenetrating networks consisting of a polymer network with dynamic cross-links and a supramolecular network allow obtaining hydrogels with significantly enhanced mechanical properties.
Experiments: Binary hydrogels composed of a dynamically cross-linked poly(vinyl alcohol) (PVA) network and a transient network of entangled highly charged mixed wormlike micelles (WLMs) of surfactants (potassium oleate and *n*-octyltrimethylammonium bromide) were prepared and studied by rheometry, SANS, USANS, cryo-TEM, and NMR spectroscopy.
Findings: Binary hydrogels show significantly enhanced rheological properties (a 3400-fold higher viscosity and 27-fold higher plateau modulus) as compared to their components taken separately. This is due to the microphase separation leading to local concentrating of PVA and WLMs providing larger number of polymer–polymer contacts for cross-linking and longer WLMs with more entanglements. Such materials are very promising for the application in many areas, ranging from enhanced oil recovery to biomedical uses.

1. Introduction

Surfactants can form very long wormlike micelles (WLMs), which can entangle with each other thereby imparting viscoelastic properties to solutions [1–5]. Since the micellar chains are formed by non-covalent interactions between surfactant molecules, they represent dynamic systems, which constantly break and reassemble [1–5]. In particular, they demonstrate low viscosity at pumping and fast and complete recovery of viscoelastic properties at rest, which is highly required, for instance, in oil industry. Also, such dynamic systems possess self-healing ability and excellent responsiveness to external triggers such as temperature, pH, various additives like salt or hydrocarbons [5–11]. However, for many applications they require enhancement of viscoelasticity.

A promising way to increase the viscoelastic properties of wormlike surfactant micelles consists in their combination with polymeric chains [12–21]. Previously, for this aim mainly macromolecules interacting with WLMs were used including macromolecules oppositely charged with respect to micelles [15,19,20] or macromolecules bearing hydrophobic side [12,13] or end [16,17] groups that penetrate the micellar interior. To provide a significant increase of viscoelasticity the fraction of polymer groups interacting with the micelles should not be too high in order to ensure only the bridging between WLMs, while keeping a significant part of polymer chains in water. Otherwise, polymers strongly interacting with WLMs can wrap around cylindrical micelles and destroy them [18,22].

Recently a new approach for the enhancement of viscoelastic properties of WLMs was proposed [23,24]. It consists in the use of polymer non-interacting (or weakly interacting) with micellar chains, which can form its own network in the whole volume of the solution independently of the micellar network. The proof of concept was made on an example of highly charged mixed WLMs of potassium oleate and *n*-octyltrimethylammonium bromide C_8TAB (at the excess of potassium oleate) and uncharged polymer - poly(vinyl alcohol) (PVA). In this system, highly charged WLMs were used to maintain the phase compatibility with the polymer, since demixing is highly unfavorable for their counterions, which need to move in a large total volume of the solution in order to gain in the translational entropy. It was demonstrated that addition of polymer can induce a 100-fold viscosity increase of the WLM solution [23,24]. Note that this effect was achieved even for uncross-linked polymer.

One can expect that the cross-linking of polymer will further enhance the viscoelasticity. However, it could reduce the responsive properties of the system and its ability to recover from suffered damage. This problem could be avoided by using dynamic (reversible) [25] rather than irreversible chemical cross-links. Dynamic covalent cross-links of PVA chains can be formed by borate ions (Scheme 1) [26–29]. The activation energy for breaking the four boronic ester bonds composing individual PVA-borate cross-link is of ca. 25 kJ/mol [26]. Such weak cross-links are reversible, they continuously break and reform. At room temperature, the PVA-borate network has a relaxation time of only 0.1–0.3 s [26,28]. The short relaxation time and low energy required to break the cross-links impart dynamic character to the whole polymer network. The dynamic-covalent nature of the boronic ester cross-links allows the system to reconfigure its covalent structure in response to external stimuli being otherwise stable. The reversibility of boronic ester linkages has been used to design self-healing polymers [30,31], sensors [32], flexible supercapacitors [33] and so forth. So, as compared to WLMs being essentially supramolecular assemblies, the PVA network will behave as covalent structure, while keeping dynamic and reversible character.

In the present paper, we report, for the first time to our knowledge, the preparation of hydrogel consisting of a transient network of entangled WLMs of surfactant and a polymer network with dynamic-covalent cross-links. The surfactant network was formed by highly charged mixed WLMs of potassium oleate and C_8TAB, the polymer network was composed of PVA cross-linked by borate ions. These networks were studied by a combination of rheology to explore macroscopic properties (viscosity, elasticity etc.), small-angle neutron scattering (SANS), ultrasmall-angle neutron scattering (USANS) and cryogenic transmission electron microscopy (cryo-TEM) to follow the structural changes occurring at the microscopic level, ^{1}H NMR spectroscopy to characterize the polymer/surfactant interactions, and ^{11}B NMR spectroscopy to study the dynamic boronic ester cross-links in the PVA-borate network. We demonstrate that the polymer can induce a 3400-fold increase of the viscosity and 27-fold increase of plateau modulus of wormlike micellar solution without altering its macroscopic phase stability. The rheological properties can be effectively controlled by varying the factors (concentrations of cross-linking agent, polymer, and surfactants) influencing the chain entanglements, polymer cross-linking and the microphase separation between polymer and surfactant components. Such hydrogels with enhanced rheological properties are very promising for various

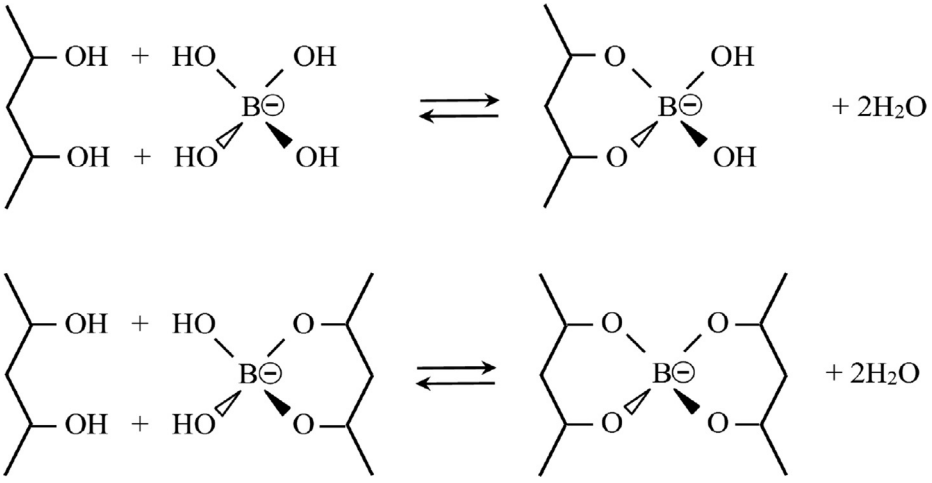

Scheme 1. Schematic representation of the interaction of polymer diol groups of PVA with borate ions, which proceeds in two steps: formation of monodiol links (I) and formation of didiol links (II).

applications, ranging from enhanced oil recovery to biomedical uses.

2. Materials and methods

2.1. Materials

Polymer PVA Mowiol 4–98 with 1.6 % residual vinyl acetate units and a molar mass of 27000 g/mol (degree of polymerization N ≈ 600) was used as received from Aldrich. Its overlap concentration C* in water was estimated as 3.2 wt% (0.7 monomol/L) from the inverse value of the intrinsic viscosity [23]. Anionic surfactant potassium oleate (purity > 98%) from TCI and cationic surfactant C_8TAB (purity > 98%) from ABCR were used without further purification. Cross-linking agent – potassium borate - was prepared by adding equimolar amount of potassium hydroxide (Acros, purity > 99.9%) to boric acid (Acros, purity > 99.8%). Distilled water was purified by the Millipore Milli-Q system, D_2O of 99.9% or 99.96% isotopic purity was supplied by Deutero GmbH or Sigma-Aldrich, respectively.

2.2. Sample preparation

Stock solution of PVA (9.2 wt%) was prepared as follows. Polymer powder and water were mixed in a round-bottom flask and slowly heated to 90 °C under reflux condenser, and after that the dissolution was carried out for 1 h while stirring. Then the solution was cooled down to room temperature. pH of PVA stock solution after preparation was equal to ~ 6. Then, 5 M KOH was added to adjust pH to 10.8, and the solution was left overnight to allow full hydrolysis of PVA acetate units to proceed. Polymer/surfactant samples were prepared by mixing stock solutions of PVA, cross-linker and surfactants at the required concentrations using a magnetic stirrer and left to equilibrate at room temperature for several days before measurements to remove air bubbles. Before mixing, pH of each of the stock solutions was adjusted to 10.8 with KOH. The concentration of surfactants was varied from 0 to 7.9 wt%. In all samples, the surfactant blend molar ratio [C_8TAB]/[potassium oleate] was set to 0.4. The concentration of PVA ranged from 1 wt% (dilute regime) to 7 wt% (semidilute unentangled regime). The molar fraction of potassium borate with respect to PVA repeat units p was varied from 0 to 0.1.

2.3. Phase behavior

The phase behavior of PVA/surfactant systems before and after cross-linking by borate was studied by visual inspection of the samples. The mixtures are considered as homogeneous if they do not show any sign of phase separation 14 days after preparation. No further evolution was observed at times as long as 60 days.

2.4. NMR spectroscopy

^{1}H NMR measurements were performed with a Bruker AV-600 spectrometer at 30 °C in D_2O as a solvent. The samples were prepared at pD = 11.2 [34] and put into standard 5-mm quartz tubes (Norell). ^{1}H chemical shifts were referenced to the HOD signal. The data were processed using ACD Labs software, including phase, baseline and reference correction.

^{11}B NMR spectra were recorded with Agilent 400 MR spectrometer operating at 128.32 MHz using quartz tubes and an external boron trifluoride etherate reference (25 % $BF_3{\cdot}O(C_2H_5)_2$ in $CDCl_3$) in a sealed capillary tube. Samples were prepared at pH = 10.8 in H_2O/D_2O mixture containing 20 wt% of D_2O. Concentrations of different types of borate ions were determined by integrating the corresponding NMR signals. For unresolved lines, peak areas were determined by fitting with generalized Lorentzian functions with the software MestRenova.

2.5. Small-angle neutron scattering

SANS experiments were conducted on the YuMO spectrometer of the high-flux pulsed reactor IBR-2 [35] at the Frank Laboratory of Neutron Physics, Joint Institute for Nuclear Research (JINR), Dubna, Russia and at the instrument D11 [36] of the Institute Laue-Langevin (ILL) in Grenoble, France. The measurements were performed at room temperature. The samples in D_2O were prepared at pD 11.2. The low viscous samples were studied in 2 mm quartz cells (Hellma, Germany). Viscous samples were measured in sandwich-type dismountable cells consisting of two round quartz windows separated by teflon spacers of 1.45- or 2-mm thickness. The data are presented as the intensity I versus the scattering vector q, where $q = (4\pi/\lambda)\sin(\theta/2)$ (λ and θ are wavelength and scattering angle, respectively).

At JINR, the data were recorded in the range of scattering vectors q of 0.005–0.7 Å^{-1} using a two-detector system. The details of the experiments are described elsewhere [37,38]. The raw spectra were corrected for background from the solvent, sample cell, and electronic noise by conventional procedures [39]. The scattered intensities were then converted to absolute scale using a calibration of primary beam detector with vanadium standard.

At the ILL, the sample-to-detector distances of 1.7 m, 16 m and 38 m were used to cover a q range from 7.63x10^{-4} to 0.65 Å^{-1}. The wavelengths used were 4.6 Å at 1.7 m and 16 m and 13 Å at 38 m, with a full width-half maximum (FWHM) wavelength spread of 9%. Scattered neutrons were detected on a multitube ^{3}He gas detector with a pixel size of 4x8 mm^2. Calibration to absolute scale was performed using light water (H_2O) scattering intensity. Raw data were saved in the .nxs (NeXuS) format [40] and corrected for transmission and background scattering prior to further analysis.

The scattering curves of the #PVA/surfactant mixtures and surfactants without polymer were fitted by a form-factor of a cylinder using the program SasView. Other models (sphere, lamellae) were also employed, but the best fits were obtained with a cylindrical model. For fitting, only a part of the curve at intermediate and high q > 0.06–0.07 Å^{-1} (higher than the structure peak position q*) was used, and then the fit was reconstructed in the whole q-range. Two fitting parameters were used: radius and length of the cylinder. However, in all cases, the length of the cylinder obtained from the fit was much larger than the accessible q-range (in the order of 2000–3000 Å). The scattering curve of the #PVA gel was fitted by a generalized Ornstein-Zernike model [41]

$$I(q) = \frac{I(0)}{\left\{1 + \left[\frac{D+1}{3}\right]\xi^2 q^2\right\}^{D/2}} \quad (1)$$

where ξ is the correlation length of the polymer network, q – scattering vector, D – fractal dimension of the network.

2.6. Cryogenic transmission electron microscopy

Cryo-TEM studies were carried out in bright field TEM on a Titan Krios 60–300 TEM/STEM (FEI, Oregon, USA) operating at 300 kV. The micrographs were obtained in low dose mode with total electron dose of less than 15 e/Å^2. Digital Micrograph (Gatan, USA) and TIA (FEI, USA) softwares were used for the image processing. The specimens were applied directly onto the Lacey carbon-coated side of the 300-mesh copper grid manually via the side port of the Vitrobot (FEI, USA) using a pipette. Then the grid was blotted to remove excess solution and immediately plunged into a reservoir with liquid ethane cooled by liquid nitrogen.

2.7. Rheometry

Rheological measurements were performed with a stress-controlled rotational rheometer Anton Paar Physica MCR 301 with cone-plate geometry (diameter 50 mm, cone angle 1^0) at 20.00 ± 0.05 ^{0}C. The details of the measurements are described elsewhere [42–44]. A specially constructed solvent trap was used to minimize water evaporation from the sample in the measuring cell.

In oscillatory shear experiments, a small-amplitude sinusoidal shear that do not disturb the structure was applied to measure the dependences of the storage G' (ω) and loss G″ (ω) moduli on the angular frequency ω of the sinusoidal deformation. The measurements were conducted in the linear viscoelastic regime, which was preliminarily determined from amplitude sweep tests at ω = 10 rad/s, so that the G' and G″ values were independent of the deformation amplitude. The frequency ω of the deformation was varied in the range of 10^{-1} to 10^2 rad/s. In steady shear experiments, the shear rate dependences of the viscosity (flow curves) were measured, the shear rate being varied from 10^{-2} to 10^3 s^{-1}. The zero-shear viscosity (η_0) was determined by extrapolating the viscosity to zero shear rate.

3. Results and discussion

3.1. Phase behavior

The system under study consists of PVA chains cross-linked by borate (#PVA) and mixed WLMs of two oppositely charged surfactants potassium oleate/C_8TAB (the length of micelles reaches few micrometers [23,45]). To reveal possible attractive interactions between the #PVA and the WLMs, ^{1}H NMR spectroscopy was used. This technique permits to detect the shift of the peaks of the groups involved in the interactions like it was shown for WLMs forming complexes with neutral [46] and oppositely [20] charged polymers. However, in the present case, the chemical shifts in the #PVA/surfactant system do not differ from those of its components (#PVA and surfactants) taken separately (Figure S1) indicating that the #PVA and the WLMs do not exhibit any attractive interactions or close contact with each other. Similar to the mixture of two slightly incompatible polymers [47], this system should have a tendency to segregative phase separation, when each phase is enriched in one of the components. Moreover, for PVA water is nearly theta-solvent (polymer–solvent interaction parameter χ = 0.494 at 30 °C [48]), which enhances the tendency for demixing in this solvent. To avoid demixing we used highly charged WLMs containing large excess of anionic surfactant with respect to C_8TAB (the molar ratio [C_8TAB]/[potassium oleate] was fixed at 0.4) without added salt. In this case, only counterions of the surfactants and of the cross-linker contribute to the ionic strength, which can be estimated [49] as 55 mM at 3.3 wt% of surfactants (for the details of the estimation see Supplementary Materials). At this low ionic strength, the highly charged micelles prevent macrophase separation, because it would lead to accumulation of almost all WLMs together with their counterions in only one phase, which is unfavorable, since it significantly reduces the translational entropy of counterions. The obtained phase diagram (Figure S2) shows that at these conditions the #PVA/surfactant system is macroscopically homogeneous in a wide range of concentrations of polymer and surfactants.

The study of the phase behavior permitted to select the conditions corresponding to the compatibility of the components, further experiments were performed only with macroscopically homogeneous samples.

3.2. Polymer cross-linking

Borate ions link to PVA 1,3-diol groups via two successive reactions [27] represented in Scheme 1. The first stage (formation of monodiol links) results in the incorporation of charged groups in the neutral polymer chain, the second stage leads to the cross-linking of polymer chains. The cross-links are mainly intramolecular in dilute solutions and both intra- and intermolecular in semi-dilute regime [50].

Therefore, in PVA-borate system, three types of borate ions can be present: free ions (B), ions linked to one *cis*-diol group (B-P), ions linked to two *cis*-diol groups (P-B-P). ^{11}B NMR spectroscopy permits to directly determine the concentration of each of these types of borate ions [27,51], since they have different chemical shifts. Fig. 1a shows the typical ^{11}B NMR spectrum of PVA – borate system. Three peaks can be identified. The downfield peak (5.7 ppm) corresponds to free boron species which are not linked to polymer chains. The position of this peak depends significantly on pH determining the relative amount of free boric acid $B(OH)_3$ (δ_B = 19.3 ppm) and free borate ions $B(OH)_4^-$ (δ_{B^-} = 1.6 ppm) which exchange fast with each other (on the ^{11}B NMR timescale) yielding a single average signal with the position δ_f depending on the relative amount of $B(OH)_3$ and $B(OH)_4^-$ species [27]:

$$B(OH)_3 + OH^- , B(OH)_4^-$$

From this peak position δ_f one can estimate pH in the system as [52]:

$$pH = \log X + pK_a$$

where $X = (\delta_f - \delta_B)/(\delta_{B^-} - \delta_f)$. The estimation using the chemical shift of the peak of free boron species (δ_f = 5.7 ppm) and pKa of potassium borate in the presence of 2 wt% PVA (pKa = 9.7 [52]) gives pH value of 10.2, which is not too far from the experimental one (pH = 10.8). At these conditions, the fraction of borate anions $B(OH)_4^-$ in the total amount of free boron species ($B(OH)_3$ + $B(OH)_4^-$) is equal to 0.77.

The other two peaks at 1.67 and 1.16 ppm correspond to borate ions linked to polymer: to one (B-P) and two diol groups (P-B-P) of PVA, respectively [27].

Figures S3a and 1c demonstrate the effect of the concentration of PVA on ^{11}B NMR spectra of #PVA/surfactant system and on the fraction of various boron species, respectively. The fraction of various boron species was determined by decomposition of the spectra into individual peaks and their integration. One can see (Fig. 1c) that when the concentration of polymer increases (at keeping constant borate/polymer ratio and surfactant concentration), the fraction of free borate ions diminishes and becomes as small as 0.04 already at 2 wt% PVA. Simultaneously the fractions of bound borates (P-B and P-B-P) rise to 0.96 imparting pronounced degree of charging to polymer chains. Among two types of bound species the B-P ones are always predominant, but at higher polymer concentration (6 wt%) they start to diminish, since a larger number of P-B-P cross-links is formed. It may be explained by increased number of polymer–polymer contacts, which can participate in cross-linking.

^{11}B NMR data can be used for quantitative evaluation of the number of borate cross-links. For instance, at 4 wt% PVA B-P-B bound boron producing the cross-links accounts for 27% of total boron. Note that B-P-B cross-links can be either intra- or intermolecular [50]. Since PVA is a flexible polymer, even when it forms a gel the fraction of intramolecular cross-links may be largely predominant. For instance, theoretical estimation [50] shows that at PVA concentration equal to 2C* the ratio of inter- to intramolecular cross-links should be only 18%.

Figure S3b demonstrates that with increasing molar fraction of cross-linker (at constant polymer and surfactant concentrations)

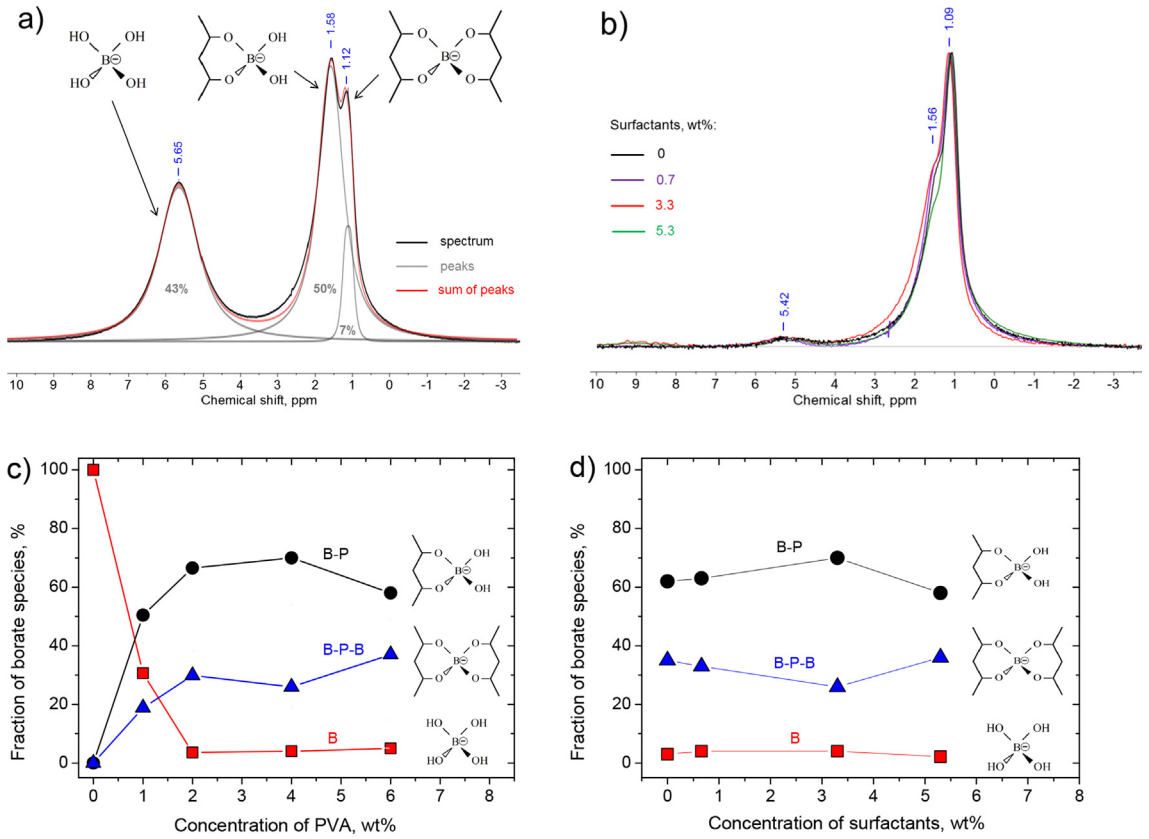

Fig. 1. (a) ^{11}B NMR spectra of #PVA containing 4 wt% PVA and 0.091 M potassium borate (molar fraction of borate with respect to PVA repeat units p = 0.1) at 30 ^{0}C and their decomposition into individual bands. (b) Effect of surfactant concentration on ^{11}B NMR spectra of #PVA/potassium oleate/C_8TAB system. Total concentrations of surfactants: 0 wt% (black), 0.7 wt% (violet), 3.3 wt% (red) and 5.3 wt% (green) at [C_8TAB]/[potassium oleate] = 0.4, 4 wt% PVA and 0.018 M potassium borate (p = 0.02). (c) Fractions of three types of borate ions: free ions (B, red squares squares), ions linked to one diol group (B-P, black circles circles), ions linked to two diol groups (P-B-P, blue triangles triangles) determined from ^{11}B NMR spectra as a function of PVA concentration for #PVA/potassium oleate/C_8TAB system containing 2.5 wt% potassium oleate, 0.8 wt% C_8TAB, and molar fraction of borate with respect to PVA repeat units p = 0.02. (d) Fractions of three types of borate squares ions: free ions (B, red squares circles), ions linked to one diol group (B-P, black circles), ions triangles linked to two diol groups (P-B-P, blue triangles) determined from ^{11}B NMR spectra as a function of total concentration of surfactants for #PVA/potassium oleate/C_8TAB system containing 4 wt% PVA at molar fraction of borate with respect to PVA repeat units p = 0.02 and molar ratio [C_8TAB]/[potassium oleate] = 0.4.

the fraction of free borate ions becomes higher, whereas the fraction of borates linked to polymer diminishes, which is in accordance with the literature data [48,50] for #PVA (without surfactant). This behavior is attributed to the fact that the binding of large amount of borate ions to PVA makes polymer chains highly charged, which hinders further attachment of borate ions due to electrostatic repulsion [50]. Such effect is more pronounced at low ionic strength [51], like in the system under study.

Fig. 1b shows that in the presence of WLMs the spectra do not change significantly. The integration of the appropriate peaks in the ^{11}B NMR spectra evidences that at fixed amount of polymer and potassium borate the surfactant concentration does not influence appreciably the fraction of different boron species (Fig. 1d) and the position and the half-width of the individual peaks (Figures S3c,d). It may be related to small number of contacts between PVA and WLMs because of their microsegregation in the #PVA/surfactant system. This assumption is in accordance with SANS data and cryo-TEM reported below. The absence of influence of surfactant concentration to the ^{11}B NMR spectrum indicates also that there is no interaction between borate ions and WLMs.

3.3. Structure revealed by SANS

3.3.1. General behavior

To reveal the structure of the system SANS studies were performed. In these experiments, D_2O (with pD adjusted to 11.2 by adding KOH) was used as a solvent. The scattering length densities of the components of the system are shown in Figure S4a. It is seen that among all components, the alkyl tails of the surfactants have the highest contrast in D_2O. In addition, WLMs are much bigger and thicker objects than PVA macromolecules. As a result, the surfactant micelles mainly contribute to the scattering when they are mixed with PVA, as is evident from Fig. 2a.

Fig. 2a presents the scattering curve of cross-linked #PVA/surfactant system in comparison with its components: surfactant solution and #PVA. It is seen that the cross-linked polymer affects mainly the low-q region (q less than 0.055 Å^{-1}), whereas at higher *q* the scattering of #PVA/surfactant system remains the same as for pure surfactant. The higher-q part of the scattering curves can be well fitted by a form-factor of cylinder (solid line, Fig. 2a) with a radius of 18.6 Å, which is close to the length of oleate tail (19 Å [9,42]). Therefore, the addition of #PVA does not affect the local cylindrical structure of micellar aggregates.

The scattering curve of #PVA in the absence of surfactants is well fitted by the generalized Ornstein-Zernike model which describes scattering from polymer gels and was previously applied for PVA/borate gels [41]. Fractal dimension D = 2.06 derived from the model, as well as the slope of the scattering curve equal to −1.9 indicate that PVA chains in the cross-linked gel are in θ-conditions. In PVA gels with significant hydrogen bonding, the values of D were reported to be somewhat larger – 2.6–2.8 [41]. This allows one to suggest that in the present system, mostly borate

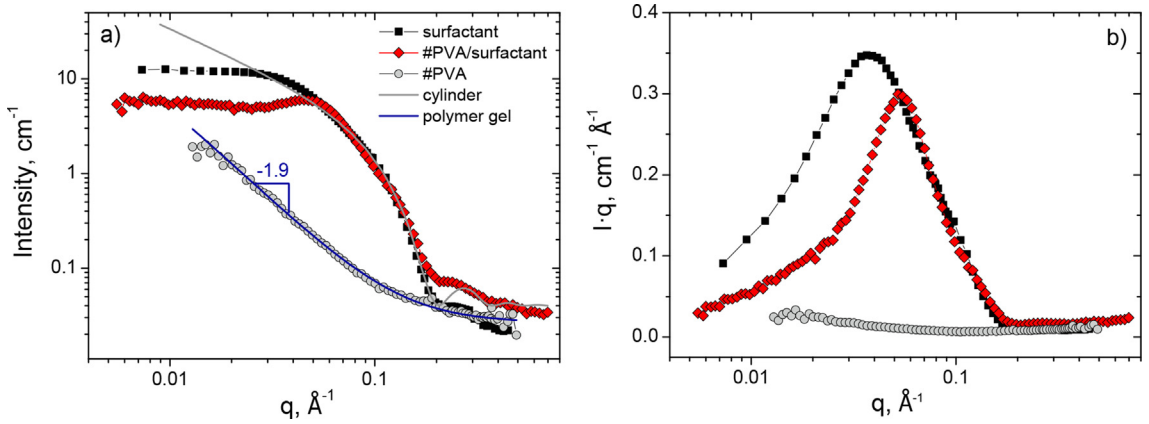

Fig. 2. The scattering curves in I (q) (a) and I·q (q) (b) coordinates for #PVA/potassium oleate/C_8TAB system cross-linked with borate (red diamonds) and its components: potassium oleate/C_8TAB solution (black squares) and #PVA (grey circles) in D_2O. Concentrations: 4 wt% PVA, 2.5 wt% potassium oleate, 0.8 wt% C_8TAB, 0.018 M potassium borate (molar fraction of borate with respect to PVA repeat units – 0.02). Grey line is a fit of the scattering curves by a form-factor of cylinder with radius R = 18.6 ± 0.2 Å. Blue line is a fit of the scattering curve by a generalized Ornstein-Zernike (gel) model with mesh size ξ = 26 nm and fractal dimension D = 2.06.

cross-links, and not hydrogen bonds, determine the structure of the #PVA network.

The curves of #PVA/surfactant system and surfactant alone demonstrate a peak at a characteristic q* value, which is clearly seen (Fig. 2b) when the scattering data are presented as I·q versus q (Holtzer plot [54]), since the multiplication of I by q allows eliminating the impact of the form factor of cylinder, which scales as $I \sim q^{-1}$ (at $qR \ll 1$) [55]. The scattering peak may be assigned to positional correlations arising from electrostatic repulsion between similarly charged micelles [56,57]. The average distance between the micelles can be estimated as $d = 2\pi/q^*$. From Fig. 2b one can see that in the presence of #PVA the peak shifts to higher q indicating that the micelles come closer to each other (although the concentration of surfactant does not change). It may occur if the micelles are expelled from the area occupied by the polymer, indicating the microsegregation with the formation of surfactant-enriched areas. So, in the systems with fixed concentration of surfactants, the shift of the q* value can be considered as an indicator of microphase separation.

3.3.2. Effect of polymer concentration

Fig. 3 demonstrates the effect of PVA concentration (at constant amount of surfactants and molar fraction of cross-linker) on the scattering curves. One can see that upon gradual addition of polymer the interaction peak arising from the mutual ordering of surfactant molecules shifts to higher q values (Fig. 3a). From the positions of the peak q* (Fig. 3a, inset) one can estimate that when PVA concentration rises from 0 to 6 wt%, the average distance d between the micelles diminishes from 166 to 106 Å. It results from increased volume occupied by polymer microphase in the microphase separated system.

The local surfactants concentration in #PVA/surfactants system was estimated under the assumption that it is equal to the concentration of surfactants solution (without polymer) having the same peak position q* characterizing the distance between the micelles. Fig. 3b shows how the effective surfactant concentration increases upon addition of polymer. For instance, in the presence of 4 wt% PVA the effective concentration of the surfactants equals to 8 wt %, which is 2.4-fold higher than in the absence of PVA (3.3 wt%). It may indicate that the surfactant microphase occupies ca. 42% of the system, whereas the PVA microphase resides in the remaining ca. 58% of the volume (Fig. 3c) if we assume a complete segregation between the components.

From the amount of added polymer and the volume of polymer-rich microphase the effective concentration of PVA in polymer microphase was estimated. It was shown (Fig. 3b) that the effective concentration of PVA is almost two-fold higher than the average concentration of polymer calculated with respect to the whole volume of the system.

To get more information about the structure of the microphase separated system at large scale the USANS studies covering quite low scattering vectors from 0.00076 Å^{-1} were performed [58]. The results are presented in Fig. 3d. It is seen that the USANS curves for #PVA/potassium oleate/C_8TAB systems demonstrate a strong upturn at low q. It may be taken as a farther indication of the formation of microphase separated domains, possibly co-continuous. With increasing polymer concentration, the scattering at low q increases. Strong upturn of the scattered intensity at low q (slope > 3) has been reported for micro-heterogeneous systems as, for instance, polymer melts [59], percolated nanoemulsion colloidal gels [60] and bicontinuous nanoparticle gels obtained by solvent segregation [61,62]. In the later system, only the nanoparticle-rich phase is expected to contribute to the viscoelastic behavior.

In our system, the observed microphase separation can result from the competition between the short-range segregation of polymer and surfactant components and long-range stabilization related to the presence of a large number of counterions neutralizing the charge of micellar chains. The microdomain structure propagating through the whole system does not impede counterions to travel in most of the volume of the solution thus ensuring the gain in their translational entropy. At the same time, it does not hinder the local segregation of incompatible polymer and surfactant components resulting in the gain in energy. The microphase separation was considered as a universal feature of polyelectrolyte systems that occurs in all cases when there are trends to component segregation at smaller scales and stabilization by the long-range factor preventing total demixing [63]. The microphase separation has been studied in many systems including mixtures of charged and neutral polymers [64], mixtures of two likely charged polyelectrolytes with different amount of charge [63], stoichiometric blends of oppositely and weakly charged polyelectrolytes, which would be immiscible in the absence of charged units [65,66], copolymer networks [67,68] and interpenetrating polymer networks [69]. It was shown theoretically that the size of the microphase separated domains in polyelectrolyte systems is determined mainly electrostatically [66]. For instance, increasing charge density of polymer chains reduces the size of microdomains, whereas added salt favors their growth [65]. As to the morphology of the microphases, increasing incompatibility between polyelectrolytes and less asymmetrical composition of the blend

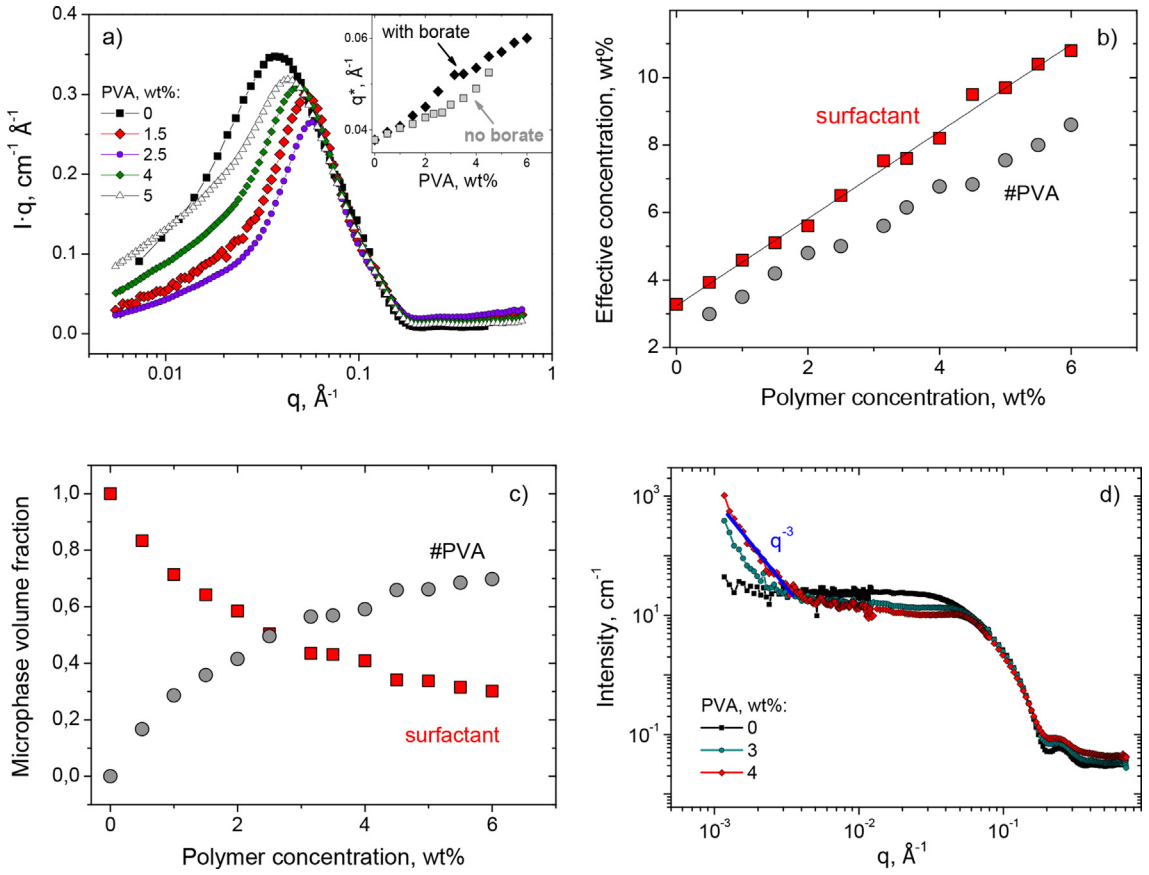

Fig. 3. (a) Scattering curves in I·q vs q representation for cross-linked #PVA/potassium oleate/C_8TAB system in D_2O in the presence of increasing amounts of PVA: 0 wt% (squares), 1.5 wt% (triangles), 2.5 wt% (diamonds), 4 wt% (red diamonds), 5 wt% (circles) at 20 °C. In the inset: Position of the correlation peak q* as a function of polymer concentration for the same system. (b,c) The effective surfactant and polymer concentrations (b) in the corresponding microphases and volume fraction of each microphase (c) calculated from the effective surfactant concentration values as a function of polymer concentration for the same system. The effective surfactant concentration in #PVA/potassium oleate/C_8TAB system was estimated as the concentration of potassium oleate/C_8TAB (without polymer) having the same peak position q*. The effective polymer concentration was estimated from the amount of added polymer and the volume of polymer-rich microphase. (d) USANS curves for cross-linked #PVA/potassium oleate/C_8TAB system in D_2O in the presence of increasing amounts of PVA: 0 wt% (squares), 3 wt% (circles), 4 wt% (diamonds) at 20 °C. Concentrations: 2.5 wt% potassium oleate, 0.8 wt% C_8TAB, molar fraction of potassium borate with respect to PVA repeat units – 0.02.

trigger the usual cascade of transitions body-centered cubic lattice of spheres → hexagonally packed cylinders → gyroids → lamellae [63–65]. The peculiarity of the present system in comparison with the polymer blends or interpenetrating networks studied previously is that one of the components is composed of non-covalent chains.

3.3.3. Effect of cross-linker concentration

The effect of cross-linker concentration on the scattering data (at fixed content of polymer and surfactants) is illustrated in Fig. 4a and S4c. It is seen that an increased amount of cross-linker leads to the shift of the correlation peak to higher q values indicating that the WLMs come closer to each other. It may be due to the charging of polymer chains as a result of linking of the borate ions which leads to the expansion of macromolecules and swelling of polymer microphase at the expense of the surfactant microphase. Note that in the presence of cross-linker the scattering intensity in 0.005–0.03 Å^{-1} q region decreases. Such behavior can be attributed [70,71] to the enhanced repulsive interactions between the WLMs, which are forced to come closer to each other in a smaller volume of the surfactant microphase.

3.3.4. Effect of surfactant concentration

Fig. 4b shows the effect of surfactant concentration on the scattering curves (at constant amount of polymer and cross-linker). It is seen that with increasing surfactant concentration, the correlation peak becomes higher and shifts to larger q values. The increase of the peak intensity indicates enhanced ordering of the micelles, whereas the shift to higher q values denotes shortening of the average distance between the micelles. Such behavior was previously observed for WLMs of many ionic surfactants [14,56]. For cylindrical aggregates in semidilute regime the peak position follows $q^* \sim C_{surf}^{0.5}$ scaling law [4,54,72,73] which reflects an ordered packing of rod-like scatterers. In the presence of uncross-linked PVA q* scales as $C_{surf}^{0.38}$ [23], which is rather close to the expected dependence. Surprisingly, in the presence of cross-linked polymer the peak position q* is only slightly dependent of the surfactant concentration (Figure S4d): $q^* \sim C_{surf}^{0.15}$. It means that with decreasing concentration of surfactants in #PVA/surfactants system the average distance between WLMs d ($d = 2\pi/q^*$) increases much less than it can be expected for WLMs in the presence of uncross-linked polymer. It may be explained as follows. In contrast to uncross-linked PVA, the cross-linked #PVA is charged due to bound borate ions. These charges together with the counterions lead to the swelling of the polymer microphase. When the amount of surfactants (together with their counterions) diminishes, it reduces the osmotic pressure in the surfactant-rich phase thereby allowing further expansion of the polymer microphase. As a result, the decrease of the surfactant concentration is accompanied by the contraction of surfactant microphase, which restricts the increase of the inter-

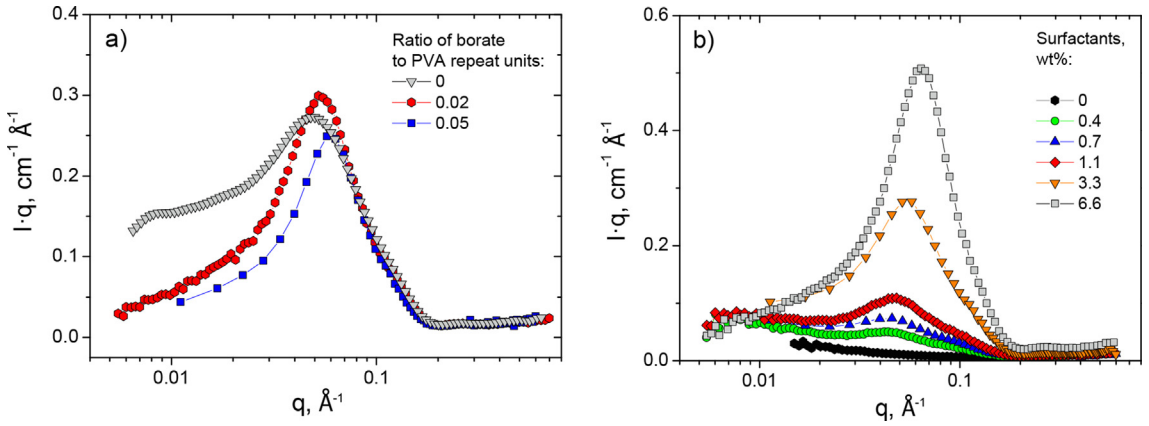

Fig. 4. (a) The scattering curves in I·q vs q coordinates for cross-linked #PVA/potassium oleate/C_8TAB systems in D_2O at 4 wt% PVA, 2.5 wt% potassium oleate, 0.8 wt% C_8TAB, and different molar fractions of borate with respect to PVA repeat units: 0 (triangles), 0.02 (diamonds), and 0.05 (squares). (b) The scattering curves in I·q vs q coordinates for cross-linked #PVA/potassium oleate/C_8TAB systems at 4 wt% PVA, 0.018 M potassium borate (molar fraction of borate with respect to PVA repeat units – 0.02) and different concentrations of the surfactants in D_2O indicated in the Figure.

micellar distances upon dilution. Note that borate ions are not expected to penetrate in the surfactant microphase, since ^{11}B NMR data show that 96% of these ions are linked to polymer both in the presence and in the absence of surfactants (Fig. 1d), whereas penetration in the surfactant microphase should lead to an increased fraction of free borate. It is important to emphasize that at high surfactant concentration exceeding 5 wt%, the cross-linked system starts to follow the behavior of uncross-linked system (Figure S4d), which may be due to enhanced screening effect of surfactant counterions.

Thus, SANS data show that added polymer network does not destroy the cylindrical structure of surfactant micelles but induces the microphase separation with the formation of polymer-rich and surfactant-rich microdomains.

3.4. Visualization of microstructure

The microstructure of #PVA/surfactants systems was visualized by cryo-TEM. From the obtained micrographs (Fig. 5) one can see a long curved microdomain of densely packed WLMs, which are mostly arranged parallel to each other. Therefore, the WLMs are preserved in the presence of polymer. Similarly arranged micellar chains were previously visualized in many WLM solutions [74,75], where they occupied the whole cryo-TEM image. By contrast, in the present system, one can observe just a large fragment of such structure representing a surfactant-rich microphase. As to polymer-rich microphase, it is suggested to cover the remaining area in the micrograph. But the PVA chains are not seen because of their very low contrast.

From Fig. 5 one can see that the average thickness of WLM microphase is ca. 80 nm. These values are of the same order as predicted theoretically for a blend of two weakly charged polyelectrolytes dissolved in the same solvent [63,64]. Within surfactant-rich microphase, one can estimate the characteristic periodicity in the packing of micellar chains as 9 nm, which is somewhat smaller than the value of the intermicellar distance d estimated from SANS correlation peak ($d = 2\pi/q^* = 12.5$ nm).

The WLMs in the surfactant-rich microphase are very long (>1 μm). At the same time, few short micelles are also observed in polymer-rich microphase. This is a clear indication of the differ-

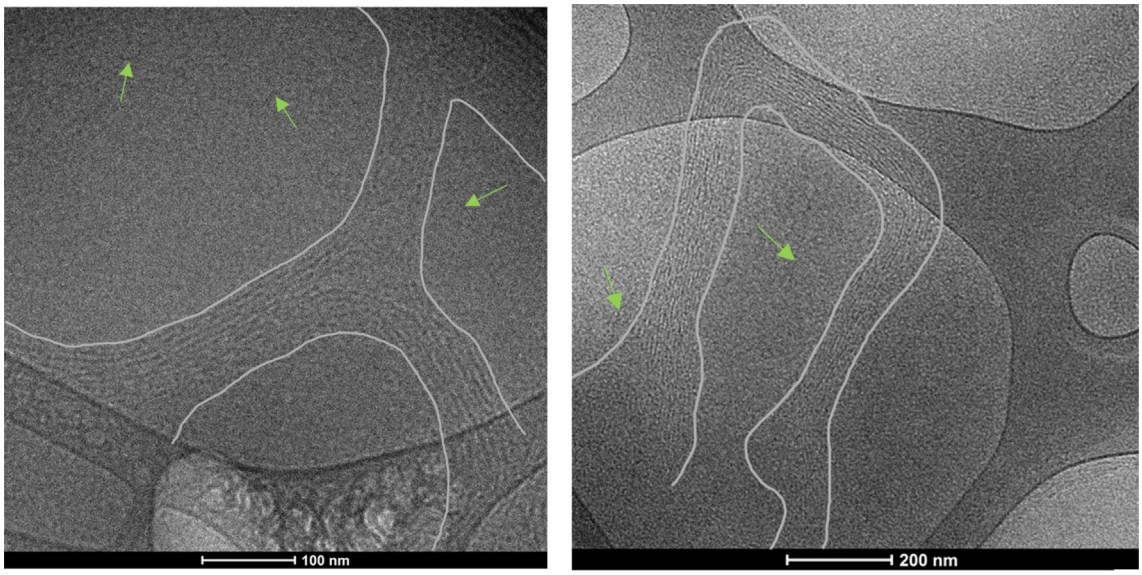

Fig. 5. Cryo-TEM pictures of cross-linked #PVA/potassium oleate/C_8TAB systems with 4 wt% PVA, molar fraction of potassium borate with respect to PVA repeat units – 0.02, 1.25 wt% oleate, 0.4 wt% C_8TAB. The boundaries of some surfactant-rich microdomains are marked by white lines, short rods are indicated by arrows.

ence of surfactant concentration in the polymer-rich and surfactant-rich microphases because the length of WLMs increases with surfactant concentration [3,5]. Thus, upon microphase separation the long micellar chains are located in surfactant-rich microphase, whereas few short micelles reside in polymer-rich microphase indicating that surfactant concentration in this microphase is very small.

Thus, cryo-TEM visualization confirms the formation of surfactant-rich and polymer-reach microphases in #PVA/surfactant system as was suggested from the analysis of SANS data.

3.5. Rheological behavior

3.5.1. General behavior

Fig. 6 shows typical results of rheological measurements for cross-linked #PVA/surfactant system and its components. It is seen that the flow curves of #PVA/surfactant system and surfactant alone demonstrate shear-thinning, which can be due to the alignment of polymer and micellar chains along the direction of flow [76]. At the same time, on the flow curve of #PVA a small region of shear-thickening is observed followed by shear-thinning. Such behavior was previously found in #PVA at polymer concentrations close to C* [51]. It was attributed to a shift from intrachain to interchain P-B-P complexes as the macromolecules elongate under shear. Note that in the presence of surfactant, the shear-thickening disappears. It suggests that the flow behavior of #PVA/-surfactant system at high shear rates (above 0.5 s^{-1}) is governed mainly by the surfactant-rich microphase which seems to be continuous and exhibits lower resistance to flow (i.e. lower viscosity). The flow curves obtained at increasing and at decreasing shear rate coincide with each other (Figure S5).

At low shear, all flow curves exhibit a Newtonian behavior, where the viscosity does not depend on the shear rate (the zero-shear viscosity η_0) and characterizes the system unperturbed by the shear. From Fig. 6 one can see that the zero-shear viscosity η_0 as well as G' and G″ values for #PVA/surfactant system are much higher than for its components. At the same time, the critical shear rate ($\dot{\gamma}_c$) corresponding to the onset of non-Newtonian thinning behavior (Fig. 6a) and the cross-over point of G'(ω) and G″(ω) dependencies (Fig. 6b) for #PVA/surfactant system are smaller than for its components indicating higher longest time of the stress relaxation.

Thus, the #PVA/surfactant system has much higher viscosity, plateau modulus and longest relaxation time than its components.

3.5.2. Effect of polymer concentration

To reveal the effect of the content of polymer on the rheological properties of the #PVA/surfactant system, we fixed the concentrations of the surfactants (2.5 wt% potassium oleate and 0.8 wt% C_8TAB) and the molar fraction of cross-linker with respect to polymer repeat units (p = 0.02). From Fig. 7a,b and S6a one can see that the viscosity, the plateau modulus, and the longest relaxation time of the #PVA/surfactant system increase with PVA concentration indicating to the formation of denser network.

At low PVA concentrations the η_0 and G_0 values of #PVA/surfactant system are determined mainly by WLMs, whereas at high PVA concentrations they are determined by the polymer network. At the same time, at the intermediate polymer content (2–4.5 wt%) a synergistic effect is observed: the mixed system has much higher η_0, G_0 and longest relaxation time τ than the sum of its components. For instance, at 3 wt% PVA the #PVA/surfactant system has a viscosity 6200 Pa·s, whereas cross-linked polymer and surfactants alone have the η_0 of 0.4 and 1.8 Pa·s, respectively (Fig. 7a). As to the plateau modulus, at 3 wt% PVA it equals to 300 Pa for the mixed system and only to 11 Pa for surfactants (Fig. 7b), whereas for polymer it even cannot be measured, since PVA does not form continuous network in the whole volume of the system in the absence of surfactants at this concentration. At these conditions, the longest relaxation time τ for the mixed system amounts to 24.4 s (Figure S6a), which is almost 500 times higher than for the surfactants (τ = 0.05 s).

Such behavior may be related to the microsegregation of polymer and micellar chains in PVA/surfactant system leading to the formation of polymer-rich and surfactant-rich domains. The local increase of the concentration of polymer chains promotes PVA cross-linking. If the cross-linked microphase separated regions are connected to each other by polymer chains, it leads to the formation of a network in the entire volume of the system. At the same time, the local increase of the concentration of micellar chains in surfactant-rich regions should induce their elongation, since the length of micelles L is known [3,5] to increase with surfactant concentration. Longer WLMs produce more entanglements. Both these effects (larger number of cross-links in the polymer-reach microdomains and larger number of entanglements in the surfactant-reach microdomains) as well as the elongation of WLMs seem to contribute to the rise of the viscosity, the plateau modulus, and the longest relaxation time.

The synergistic enhancement of η_0, G_0 and τ values is observed at the conditions when the volumes of both microphases are rather close to each other (Fig. 3c). Most probably, such conditions pro-

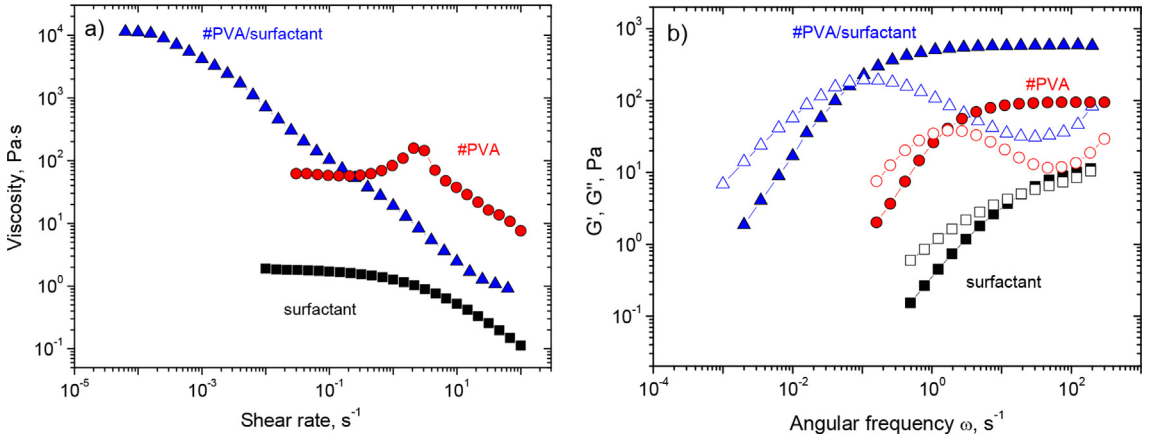

Fig. 6. Flow curves (a) and frequency dependencies of storage G' (filled symbols) and loss G″ (open symbols) moduli (b) for cross-linked #PVA/potassium oleate/C_8TAB system and its components: #PVA network and potassium oleate/C_8TAB solution at 20 °C. Concentrations: 4 wt% PVA, 0.018 M potassium borate (molar fraction of borate with respect to PVA repeat units – 0.02), 2.5 wt% potassium oleate, 0.8 wt% C_8TAB.

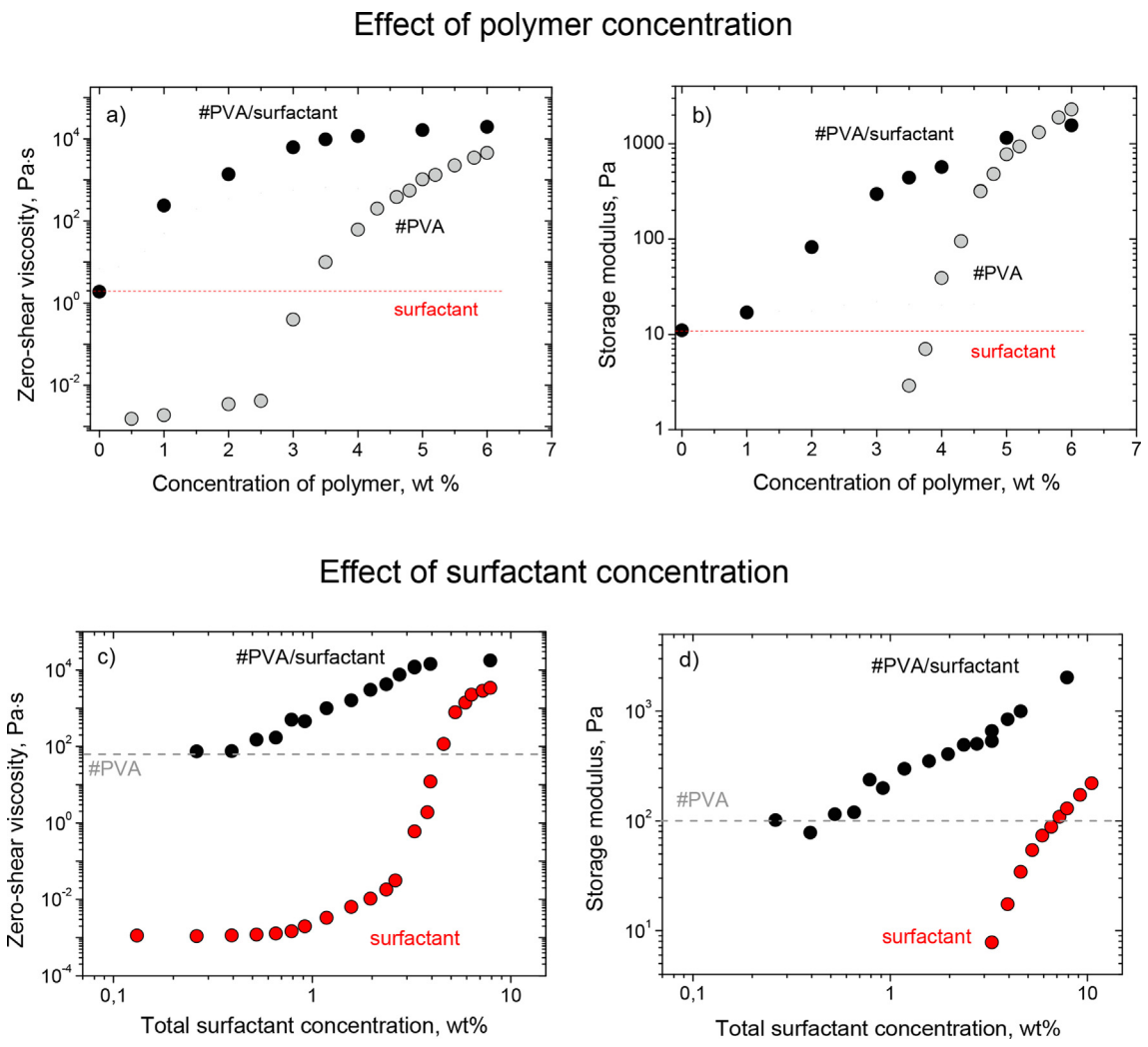

Fig. 7. (a,b) Zero-shear viscosity η_0 (a) and plateau modulus G_0 (in the absence of polymer the value of G' at ω = 120 rad/s was taken) (b) as a function of PVA concentration for cross-linked #PVA/potassium oleate/C_8TAB system (black circles) and its components: #PVA network (grey circles) and potassium oleate/C_8TAB solution (dashed line) at 20 °C. Concentrations: 2.5 wt% potassium oleate, 0.8 wt% C_8TAB, molar fraction of borate with respect to PVA repeat units p = 0.02. (c,d) Zero-shear viscosity η_0 (c) and plateau modulus G_0 (d) as a function of the total surfactant concentration for cross-linked #PVA/potassium oleate/C_8TAB system (black circles) and its components: #PVA network (dashed line) and potassium oleate/C_8TAB solution (red circles) at 20 °C. Concentrations: 4 wt% PVA, molar fraction of borate with respect to PVA repeat units p = 0.02, molar ratio [C_8TAB]/[potassium oleate] = 0.4.

vide the formation of bicontinuous microphase separated structure, so that each of the components can spread in the whole volume of the system. When the amount of one of the components becomes predominant, the synergistic effect vanishes (Fig. 7).

Note that the cross-linker represents a low-molecular-weight salt, which can enhance the viscosity by inducing the growth of WLMs in length. To estimate this effect, we compared the rheological data for potassium oleate/C_8TAB surfactant solution in the absence and in the presence of 0.72 mM sodium borate, which corresponds to the concentration of free borate (according to ^{11}B NMR data) in 4 wt% PVA with molar fraction of cross-linker equal to 0.02. It was shown that this amount of sodium borate only slightly affects the rheological curves. For instance, the zero-shear viscosity increases by 1.5-fold, whereas #PVA cross-linked with borate induces an increase of the viscosity by more than three orders of magnitude (Fig. 6a). Therefore, the effect of borate alone is very small in comparison with the effect of #PVA cross-linked by borate.

A pronounced increase of the viscosity, the plateau modulus and the longest relaxation time is observed even at the addition of rather low amount of PVA (2 wt%) when the mean PVA concentration in the system is below C^*_{PVA} (C^*_{PVA} = 3.2 wt%). This is one more indication of the local concentrating of PVA as a result of microphase separation that promotes PVA cross-linking. Indeed, according to SANS data in #PVA/surfactants systems with 2 wt% PVA the effective local concentration of polymer is equal to 4.8 wt% that is higher than the gelation concentration reported for pure PVA (4 wt% [53]).

Thus, at polymer concentrations from 2 to 4.5 wt% a huge synergistic enhancement of viscosity, plateau modulus and longest relaxation time compared to cross-linked polymer and surfactants alone is observed. It can be attributed to local concentrating of the components in each of the microphases and the spreading of the continuous microphases through the whole volume of the system.

3.5.3. *Effect of cross-linker concentration*

Fig. 8 shows the effect of cross-linking density on the rheological data (at constant concentrations of polymer and surfactants). It is seen that the viscosity and the plateau modulus increase with increasing content of cross-linker, which is expected. At the same time, the cross-linker does not appreciably affect the frequency of the intersection of G' and G″, i.e. the longest relaxation time τ. One can suggest that the longest relaxation time is determined

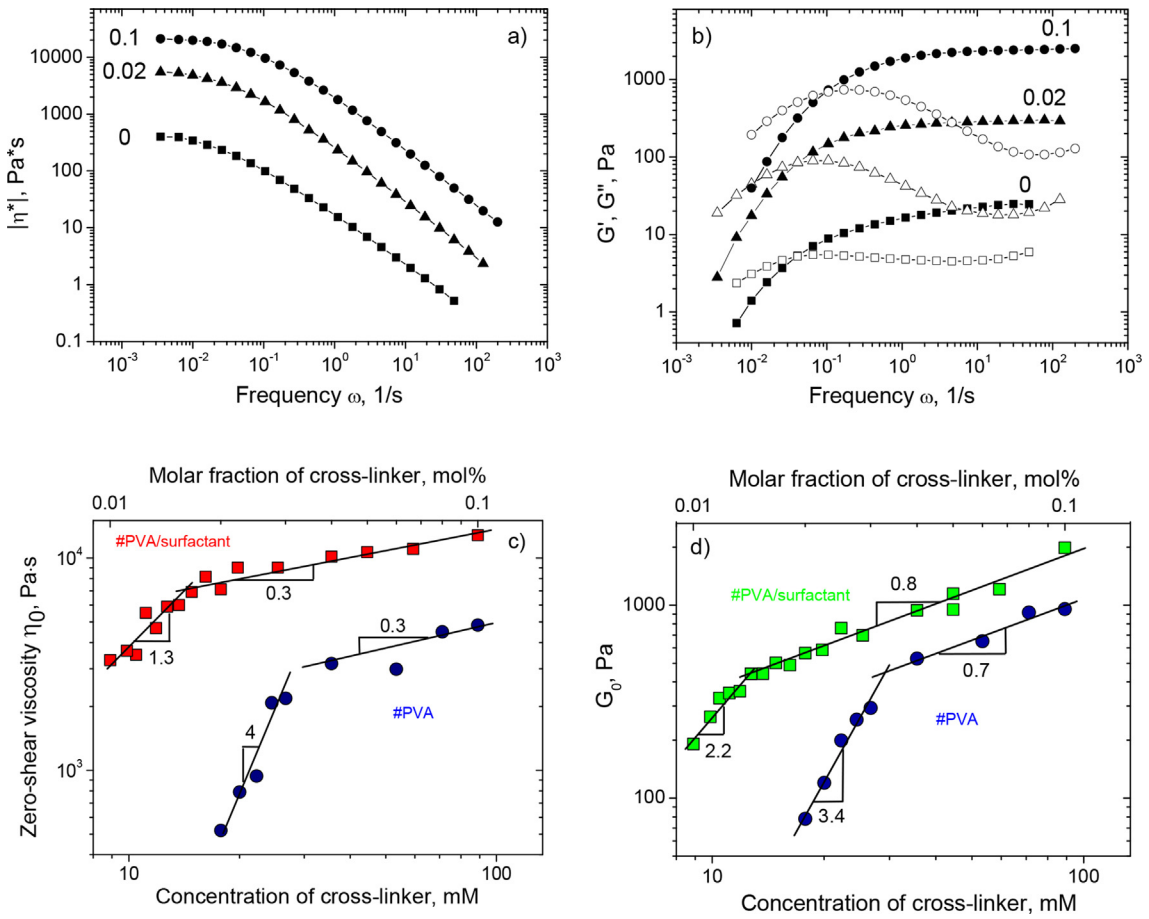

Fig. 8. (a,b) Frequency dependencies of the modulus of complex viscosity $|\eta^*|$ (a) and of the storage G' and loss G″ moduli (b) for #PVA /potassium oleate/C_8TAB system with increasing molar fraction of cross-linker (potassium borate) with respect to PVA repeat units: 0 (squares), 0.02 (triangles) and 0.10 (circles) at 20 °C. (c,d) Log-log dependencies of zero-shear viscosity (c) and plateau modulus (d) on the concentration of cross-linker (potassium borate) and the fraction of borate ions with respect to PVA repeat units. Concentrations: 2.5 wt% potassium oleate, 0.8 wt% C_8TAB, 4 wt% PVA.

mainly by the relaxation of WLMs in the mixed PVA/surfactant system and is almost independent of the dynamic cross-links between polymer chains.

Fig. 8c,d shows the variation of the zero-shear viscosity η_0 and plateau modulus G_0 with the concentration of added cross-linker C_{cr} at fixed polymer concentration close to C^*_{PVA}. At these conditions, no PVA chain entanglements are expected since the entanglement concentration C_e is usually 5–10 times higher than C^* [77]. From Fig. 8c,d it is seen that at very low molar fraction of the cross-linker (0.01–0.015) $\eta_0 \sim C_{cr}^{1.3}$ and $G_0 \sim C_{cr}^{2.2}$, whereas at higher molar fraction of the cross-linker (0.015–0.10) the increase of the zero-shear viscosity and plateau modulus is less pronounced: $\eta_0 \sim C_{cr}^{0.3}$ and $G_0 \sim C_{cr}^{0.8}$. Initial strong increase of η_0 and G_0 with borate concentration can be due to both cross-linking and chain expansion of PVA because of repulsive interactions between the bound borate ions. At higher borate concentration, when the PVA chains become strongly charged, the increase of η_0 and G_0 becomes less pronounced. It can be due to the lowering of the fraction of boron species participating in the cross-links, since cross-link formation requires the interaction of two strongly charged polyanionic chains, which repel each other. This suggestion is consistent with ^{11}B NMR data (Figure S3b), which show that the fraction of free boron augments considerably upon increasing the concentration of potassium borate. Similar two different slopes are observed (Fig. 8c,d) on the concentration dependences of η_0 and G_0 for #PVA (without surfactants). But in this case, the transition to low-sloped line is shifted to higher molar fraction of the cross-linker (from 0.015 to 0.035). Therefore, in the absence of surfactant, the strong repulsion is observed at higher charge density produced by bound borate ions. It may count in favor of our suggestion about microphase separation in the presence of surfactants, which leads to local concentrating of polymer chains, so that in fact the charge density in polymer-rich domains is higher than that estimated under assumption that polymer occupies the whole volume of the system.

Note that at high borate concentration, the plateau modulus scales as $G_0 \sim C_{cr}^{0.7\text{-}0.8}$ both in the absence and in the presence of the surfactants, whereas according to the theory of elasticity of polymer networks [78–80], the plateau modulus of the gels should scale with the concentration of cross-linker as $G_0 \sim C_{cr}^1$, since

$$G \sim \nu RT \qquad (2)$$

where ν is the concentration of elastically active subchains, R is the molar gas constant. Smaller exponent could be due to two reasons: (i) lowering fraction of borate ions participating in cross-links, which is clearly seen on ^{11}B NMR data (Figure S3b), and (ii) formation of some loops, which do not contribute to the elasticity.

Figure S7 allows estimating the effect of cross-linking by comparing cross-linked and uncross-linked PVA/surfactant systems. It is seen that in both systems, the viscosity and the plateau modulus increase with PVA concentration, but in the cross-linked system the effect of polymer is much more significant. Figure S7d summarizes the influence of polymer cross-linking on different rheological properties (η_0, G_0, and the longest relaxation time τ). One can see

that the most pronounced effect of cross-linker is observed on the plateau modulus. As compared to the uncross-linked system, the cross-linking provides a 74-fold increase of the plateau modulus G_0 and a 32-fold increase of the viscosity η_0, but almost does not affect the longest relaxation time.

Note that mixing of PVA and WLMs in the absence of cross-linker leads to very small (2-fold) increase of plateau modulus (Figure S7b). Therefore, most of the effect on the plateau modulus is due to cross-linking of polymer chains. From the difference in G_0 values for cross-linked and uncross-linked systems, it is possible to estimate the number of new elastically active chains caused by PVA cross-linking by potassium borate. For example, at 4 wt% PVA and 0.018 M potassium borate this difference is equal to 530 Pa, which corresponds to $2.2x10^{-4}$ M elastically active chains according to eq.(2). At the same time, the amount of added cross-linker (0.018 M borate) provides $4.9x10^{-3}$ M P-B-P links, according to ^{11}B NMR data (Fig. 1d). If all of them form intermolecular cross-links, it would correspond to $9.8x10^{-3}$ M elastically active chains, since 1 cross-link gives 2 elastically active chains. However, the actual number of new elastically active chains provided by borate is only $2.2x10^{-4}$ M that is 2.2% of all P-B-P links. It may be due to small number of interpolymer contacts in unentangled regime. Therefore, ^{11}B NMR data allow estimating the total number of P-B-P contacts including intra- and intermolecular ones. But the combination with rheological data gives the possibility to determine the fraction of intermolecular contacts contributing to elasticity. Note that in the corresponding system without surfactants the percent of intermolecular cross-links contributing to elasticity (G_0 = 78 Pa) is much lower – 0.3% . Therefore, at these conditions the intermolecular cross-linking in #PVA/surfactant is more efficient than in #PVA alone. As was discussed above, it may be due to microphase separation leading to local concentrating of PVA chains trying to escape from the area occupied by WLMs.

The fact that the cross-linker does not affect the longest relaxation time τ (Figure S7c,d) suggests that this time is governed mainly by WLMs. However, the τ value for #PVA/surfactants system is much higher than for pure surfactants (Fig. 6b). Most probably it is due to larger concentration of surfactants in the surfactant-rich domains, which makes the WLMs longer and enhance their interlacing. These long WLM chains being much larger objects than the PVA macromolecules are responsible for the longest relaxation time.

As a result, in the #PVA/surfactants system, the cross-linked polymer seems to give the main input to enhanced elastic properties providing higher plateau modulus G_0, whereas the WLMs mainly contribute to large values of the longest relaxation time.

3.5.4. Effect of surfactant concentration

Let us examine the effect of the surfactant concentration on the rheological data. From Fig. 7c one can see that in potassium oleate/C_8TAB system (without polymer) a pronounced increase of the zero-shear viscosity occurs abruptly at ca. 2 wt% of surfactants, which corresponds to the overlap concentration C^*_{WLM} of the WLMs formed by the surfactant mixture under study.

In the presence of polymer, the increase of viscosity η_0, the plateau modulus G_0 and the longest relaxation time τ is observed (Fig. 7d and S6b) already at surfactant concentrations well below C^*_{WLM} (0.5–1.5 wt%), when the micelles are short rod-like (in the absence of polymer). Once again it indicates to the microphase separation leading to local concentrating of PVA and WLMs providing larger number of polymer–polymer contacts for cross-linking in the polymer-rich microdomains as well as the increase of the length of the micelles and the number of entanglements between them in the surfactant-rich microdomains.

Thus, mixing of #PVA with WLMs of surfactant induces a huge increase of viscosity, plateau modulus and longest relaxation time resulting from the local concentrating of the components in continuous microphases spreading though the whole volume of the system. Most probably, the cross-linked polymer is mainly responsible for enhanced elastic properties, whereas the WLMs mainly contribute to large values of longest relaxation time. At the same time, both components give their input in the increased values of zero-shear viscosity.

4. Conclusions

In this work, we prepared and studied a new type of double dynamic hydrogels based on a combination of highly charged WLMs and a non-ionic polymer PVA dynamically cross-linked by borate ions. Very long, entangled WLMs were formed by mixing C_8TAB with excess of potassium oleate at a molar ratio [C_8TAB]/[potassium oleate] = 0.4. Our starting hypothesis was that polymer and surfactants will form two independent networks interlaced into a bicontinuous structure as a result of the segregation between PVA-rich and surfactant-rich microdomains. Such mixtures are expected to be macroscopically homogeneous due to the presence of WLMs counterions which move in the total volume of the solution in order to gain in the translational entropy. Finally, the dynamic cross-linking of PVA by borate ions was expected to enhance considerably the rheological properties of these mixed systems.

By using NMR spectroscopy, we found that PVA does not impact the local structure of WLMs (^{1}H NMR) while the surfactant concentration does not influence appreciably the fraction of borate cross-links in the PVA microdomains (^{11}B NMR). A strong synergistic enhancement in rheological properties (zero shear viscosity, plateau modulus and longest relaxation time), as compared to cross-linked polymer and surfactants alone, was observed for PVA concentrations between 2 and 4.5%, i.e., close to the C*. The enhancement in rheological properties can be one to two orders of magnitude higher than in the corresponding uncross-linked PVA/potassium oleate/C_8TAB system [23] without losing a dynamic character of the networks.

The combination of SANS and USANS allowed the characterization of microstructure over 3 orders of magnitude in size (1 nm to 1 μm) and confirmed the microphase separation in PVA-rich and WLMs-rich domains. The microdomains were visualized by cryo-TEM. The strongest enhancement in rheological properties was observed when the volumes of both microphases are rather close to each other providing the conditions for the formation of bicontinuous microphase separated structure, so that each of the components can spread in the whole volume of the system. When the amount of one of the components becomes predominant, the synergistic effect vanishes.

This new kind of soft hydrogel materials, composed of two microphase separated networks, one consisting of dynamically cross-linked polymer chains and the other of entangled wormlike surfactant micelles, differs significantly from previously reported interacting polymer/surfactant systems. In the later, the increase in viscoelastic properties was achieved by association between the polymer and the WLMs either via electrostatic attraction (oppositely charged polymer and WLMs [15,19,20]) or via hydrophobic interaction (WLMs with polymers bearing hydrophobic side [12,13] or end groups [16,17]). In both cases the fraction of polymer groups interacting with WLMs has to be finely tuned and remain low just to ensure bridging between WLMs without inducing their destruction. On the other hand, because of their bicontinuous structure, our double dynamic hydrogels can be considered

conceptually similar to bicontinuous nanoparticle gels obtained by binary solvent segregation [61,62].

Dynamic character of the cross-links in the first network and non-covalent chains of the second network should provide to the hydrogel a responsiveness to external triggers and the self-healing ability. In particular, heating is expected to shorten the micellar chains and to disrupt partially the borate cross-links, which will be able to tune the viscoelastic properties when necessary. Further work is being carried out in our groups to explore the applicability of the double dynamic network concept to other polymer/surfactant systems [81] and evaluate their responsiveness to external stimuli and the self-healing behavior as well as the factors controlling them.

Funding

This work is financially supported by the Russian Science Foundation (project № 19-73-20133).

CRediT authorship contribution statement

Andrey V. Shibaev: Investigation, Formal analysis, Writing – original draft, Writing – review & editing. **Alexander I. Kuklin:** Investigation, Formal analysis. **Vladimir N. Torocheshnikov:** Investigation, Formal analysis. **Anton S. Orekhov:** Investigation, Formal analysis. **Sébastien Roland:** Investigation, Formal analysis. **Guillaume Miquelard-Garnier:** Investigation, Formal analysis. **Olga Matsarskaia:** Investigation, Formal analysis. **Ilias Iliopoulos:** Conceptualization, Formal analysis, Writing – review & editing, Supervision. **Olga E. Philippova:** Formal analysis, Writing – original draft, Writing – review & editing, Supervision, Funding acquisition.

Declaration of Competing Interest

The authors declare that they have no known competing financial interests or personal relationships that could have appeared to influence the work reported in this paper.

Acknowledgement

This work is financially supported by the Russian Science Foundation (project № 19-73-20133). The authors acknowledge the Joint Institute for Nuclear Research (Dubna, Russia) and the Institute Laue-Langevin (Grenoble, France, ILL proposal 9-11-2009) for the allocated neutron beam time, K.A. Abrashitova for the help with some experimental measurements and C. Sollogoub and M. Gervais for fruitful discussions. A.O. research (cryo-TEM experiments) was supported by the Ministry of Science and Higher Education. O.P. would like to express her sincere thanks to all colleagues of the laboratory Procédés et Ingénierie en Mécanique et Matériaux (Arts et Métiers, Paris, France) for their perfect hospitality and many inspiring discussions during her visit to the laboratory.

Appendix A. Supplementary material

Supplementary data to this article can be found online at https://doi.org/10.1016/j.jcis.2021.11.198.

References

[1] R. Zana, E.W. Kaler, Giant micelles: Properties and applications, CRC Press (2007), https://doi.org/10.1201/9781420007121.

[2] C.A. Dreiss, Y. Feng, Wormlike micelles: advances in systems, characterization and applications, Roy. Soc. Chem. (2017), https://doi.org/10.1039/9781782629788.

[3] L.J. Magid, The surfactant-polyelectrolyte analogy, J. Phys. Chem. B 102 (21) (1998) 4064–4074, https://doi.org/10.1021/jp9730961.

[4] M.E. Cates, S.M. Fielding, Rheology of giant micelles, Adv. Phys. 55 (7–8) (2006) 799–879, https://doi.org/10.1080/00018730601082029.

[5] C.A. Dreiss, Wormlike micelles: where do we stand? Recent developments, linear rheology and scattering techniques, Soft Matter 3 (8) (2007) 956–970, https://doi.org/10.1039/B705775J.

[6] V.S. Molchanov, O.E. Philippova, A.R. Khokhlov, Y.A. Kovalev, A.I. Kuklin, Self-assembled networks highly responsive to hydrocarbons, Langmuir 23 (1) (2007) 105–111, https://doi.org/10.1021/la061612l.

[7] O.E. Philippova, A.R. Khokhlov, Smart polymers for oil production, Petroleum Chem. 50 (4) (2010) 266–270, https://doi.org/10.1134/S0965544110040031.

[8] Z. Chu, C.A. Dreiss, Y. Feng, Smart wormlike micelles, Chem. Soc. Rev. 42 (17) (2013) 7174–7203, https://doi.org/10.1039/C3CS35490C.

[9] A.V. Shibaev, M.V. Tamm, V.S. Molchanov, A.V. Rogachev, A.I. Kuklin, E.E. Dormidontova, O.E. Philippova, How a viscoelastic solution of wormlike micelles transforms into a microemulsion upon absorption of hydrocarbon: New insight, Langmuir 30 (13) (2014) 3705–3714, https://doi.org/10.1021/la500484e.

[10] J. Jiang, D. Zhang, J. Yin, Z. Cui, Responsive, switchable wormlike micelles for CO_2/N_2 and redox dual stimuli based on selenium-containing surfactants, Soft Matter 13 (37) (2017) 6458–6464, https://doi.org/10.1039/C7SM01308F.

[11] Q.i. Liu, D. Lv, J. Zhang, C. Huang, B. Yin, X. Wei, J. Li, Triple-responsive wormlike micelles based on cationic surfactant and sodium trans-o-methoxycinnamic acid, J. Mol. Liq. 324 (2021) 114680, https://doi.org/10.1016/j.molliq.2020.114680.

[12] J.A. Shashkina, O.E. Philippova, Y.D. Zaroslov, A.R. Khokhlov, T.A. Pryakhina, I.V. Blagodatskikh, Rheology of viscoelastic solutions of cationic surfactant Effect of added associating polymer, Langmuir 21 (4) (2005) 1524–1530, https://doi.org/10.1021/la0482756.

[13] I. Couillet, T. Hughes, G. Maitland, F. Candau, Synergistic effects in aqueous solutions of mixed wormlike micelles and hydrophobically modified polymers, Macromolecules 38 (12) (2005) 5271–5282, https://doi.org/10.1021/ma0501592.

[14] C. Flood, C.A. Dreiss, V. Croce, T. Cosgrove, G. Karlsson, Wormlike micelles mediated by polyelectrolyte, Langmuir 21 (17) (2005) 7646–7652, https://doi.org/10.1021/la050326r.

[15] K. Nakamura, T. Shikata, Anionic hybrid threadlike micelle formation in an aqueous solution, J. Phys. Chem. B 110 (49) (2006) 24802–24805, https://doi.org/10.1021/jp066424i.

[16] L. Ramos, C. Ligoure, Structure of a new type of transient network: Entangled wormlike micelles bridged by telechelic polymers, Macromolecules 40 (4) (2007) 1248–1251, https://doi.org/10.1021/ma0621167.

[17] T. Yoshida, R. Taribagil, M.A. Hillmyer, T.P. Lodge, Viscoelastic synergy in aqueous mixtures of wormlike micelles and model amphiphilic triblock copolymers, Macromolecules 40 (5) (2007) 1615–1623, https://doi.org/10.1021/ma062428+.

[18] K.R. Francisco, M.A. Da Silva, E. Sabadini, G. Karlsson, C.A. Dreiss, Effect of monomeric and polymeric co-solutes on cetyltrimethylammonium bromide wormlike micelles: Rheology, cryo-TEM and small-angle neutron scattering, J. Colloid Interface Sci. 345 (2) (2010) 351–359, https://doi.org/10.1016/j.jcis.2010.01.086.

[19] I. Hoffmann, P. Heunemann, S. Prevost, R. Schweins, N.J. Wagner, M. Gradzielski, Self-aggregation of mixtures of oppositely charged polyelectrolytes and surfactants studied by rheology, dynamic light scattering and small-angle neutron scattering, Langmuir 27 (8) (2011) 4386–4396, https://doi.org/10.1021/la104588b.

[20] E. Oikonomou, G. Bokias, J.K. Kallitsis, I. Iliopoulos, Formation of hybrid wormlike micelles upon mixing cetyl trimethylammonium bromide with poly (methyl methacrylate-co-sodium styrene sulfonate) copolymers in aqueous solution, Langmuir 27 (8) (2011) 5054–5061, https://doi.org/10.1021/la200017j.

[21] H. Sharma, E.E. Dormidontova, Polymer-threaded and polymer-wrapped wormlike micelle solutions: Molecular dynamics simulations, Macromolecules 52 (18) (2019) 7016–7027, https://doi.org/10.1021/acs.macromol.9b0097410.1021/acs.macromol.9b00974.s001.

[22] X. Li, Z. Lin, J. Cai, L.E. Scriven, H.T. Davis, Polymer-induced microstructural transitions in surfactant solutions, J. Phys. Chem. 99 (27) (1995) 10865–10878, https://doi.org/10.1021/j100027a030.

[23] A.V. Shibaev, K.A. Abrashitova, A.I. Kuklin, A.S. Orekhov, A.L. Vasiliev, I. Iliopoulos, O.E. Philippova, Viscoelastic synergy and microstructure formation in aqueous mixtures of nonionic hydrophilic polymer and charged wormlike surfactant micelles, Macromolecules 50 (1) (2017) 339–348, https://doi.org/10.1021/acs.macromol.6b0238510.1021/acs.macromol.6b02385.s001.

[24] A.V. Shibaev, A.V. Makarov, A.I. Kuklin, I. Iliopoulos, O.E. Philippova, Role of charge of micellar worms in modulating structure and rheological properties of their mixtures with nonionic polymer, Macromolecules 51 (1) (2018) 213–221, https://doi.org/10.1021/acs.macromol.7b0224610.1021/acs.macromol.7b02246.s001.

[25] S. Huang, X. Kong, Y. Xiong, X. Zhang, H. Chen, W. Jiang, Y. Niu, W. Xu, C. Ren, An overview of dynamic covalent bonds in polymer material and their applications, Eur. Polym. J. 141 (2020) 110094, https://doi.org/10.1016/j.eurpolymj.2020.110094.

[26] R.K. Schultz, R.R. Myers, The chemorheology of poly(vinyl alcohol)-borate gels, Macromolecules 2 (3) (1969) 281–285, https://doi.org/10.1021/ma60009a014.
[27] E. Perzon, L. Leibler, A. Ricard, F. Lafuma, R. Audebert, Complex formation in polymer-ion solutions. 1. Polymer concentration effects, Macromolecules 22 (3) (1989) 1169–1174, https://doi.org/10.1021/ma00193a030.
[28] I.D. Robb, J.B.A.F. Smeulders, The rheological properties of weak gels of poly (vinyl alcohol) and sodium borate, Polymer 38 (9) (1997) 2165–2169, https://doi.org/10.1016/S0032-3861(96)00755-0.
[29] J. Li, X. Cao, Y. Liu, Q. Chen, Thermorheological complexity of poly(vinyl alcohol)/borax aqueous solutions, J. Rheol. 64 (4) (2020) 991–1002, https://doi.org/10.1122/8.0000043.
[30] F. Seidi, Y. Jin, J. Han, M.R. Saeb, A. Akbari, S.H. Hosseini, M. Shabanian, H. Xiao, Self-healing polyol/borax hydrogels: Fabrications, properties and applications, Chem. Rec. 20 (10) (2020) 1142–1162, https://doi.org/10.1002/tcr.202000060.
[31] J. Ai, K. Li, J. Li, F. Yu, J. Ma, Super flexible, fatigue resistant, self-healing PVA/xylan/borax hydrogel with dual-crosslinked network, Int. J. Biol. Macromol. 172 (2021) 66–73, https://doi.org/10.1016/j.ijbiomac.2021.01.038.
[32] M. Li, J.S. Fossey, T.D. James, Boron: Sensing, Synthesis and Supramolecular Self-assembly, Roy. Soc. Chem. (2015), https://doi.org/10.1039/9781782622123.
[33] K. Cicek, S. Demirel, Self-healable PVA–graphite–borax as electrode and electrolyte properties for smart and flexible supercapacitor applications, J. Mater. Sci.: Materials, Electronics 32 (12) (2021) 16335–16345, https://doi.org/10.1007/s10854-021-06186-w.
[34] P.K. Glasoe, F.A. Long, Use of glass electrodes to measure acidities in deuterium oxide, J. Phys. Chem. 64 (1960) 188–190, https://doi.org/10.1021/j100834a026.
[35] A.I. Kuklin, A.K. Islamov, V.I. Gordeliy, Scientific reviews: Two-detector system for small-angle neutron scattering instrument, Neutron News 16 (3) (2005) 16–18, https://doi.org/10.1080/10448630500454361.
[36] K. Lieutenant, P. Lindner, R. Gahler, A new design for the standard pinhole small-angle neutron scattering instrument D11, J. Appl. Cryst. 40 (6) (2007) 1056–1063, https://doi.org/10.1107/S0021889807038253.
[37] V.S. Molchanov, A.I. Kuklin, A.S. Orekhov, N.A. Arkharova, O.E. Philippova, Temporally persistent networks of long-lived mixed wormlike micelles of zwitterionic and anionic surfactants, J. Mol. Liq. 342 (2021) 116955, https://doi.org/10.1016/j.molliq.2021.116955.
[38] O.P. Artykulnyi, A.V. Shibaev, M.M. Avdeev, O.I. Ivankov, L.A. Bulavin, V.I. Petrenko, O.E. Philippova, Structural investigations of poly(ethylene glycol)-dodecylbenzenesulfonic acid complexes in aqueous solutions, J. Mol. Liq. 308 (2020) 113045, https://doi.org/10.1016/j.molliq.2020.113045.
[39] A.G. Soloviev, T.M. Solovjeva, O.I. Ivankov, D.V. Soloviov, A.V. Rogachev, A.I. Kuklin, SAS program for two-detector system: seamless curve from both detectors, J. Phys.: Conf. Ser. 848 (2017) 012020, https://doi.org/10.1088/1742-6596/848/1/012020.
[40] M. Könnecke, F.A. Akeroyd, H.J. Bernstein, A.S. Brewster, S.I. Campbell, B. Clausen, S. Cottrell, J.U. Hoffmann, P.R. Jemian, D. Männicke, R. Osborn, P.F. Peterson, T. Richter, J. Suzuki, B. Watts, E. Wintersberger, J. Wuttke, The NeXus data format, J. Appl. Cryst. 48 (2015) 301–305, https://doi.org/10.1107/S1600576714027575.
[41] M. Shibayama, H. Kurokawa, S. Nomura, M. Muthukumar, R.S. Stein, S. Roy, Small-angle neutron scattering from poly (vinyl alcohol)-borate gels, Polymer 33 (14) (1992) 2883–2890, https://doi.org/10.1016/0032-3861(92)90072-5.
[42] A.V. Shibaev, V.S. Molchanov, O.E. Philippova, Rheological behavior of oil-swollen wormlike surfactant micelles, J. Phys. Chem. B 119 (52) (2015) 15938–15946, https://doi.org/10.1021/acs.jpcb.5b10505.
[43] O.E. Philippova, A.V. Shibaev, D.A. Muravlev, D.Y. Mityuk, Structure and rheology of solutions and gels of stiff polyelectrolyte at high salt concentration, Macromolecules 49 (16) (2016) 6031–6040, https://doi.org/10.1021/acs.macromol.6b0139210.1021/acs.macromol.6b01392.s001.
[44] A.S. Ospennikov, A.A. Gavrilov, O.P. Artykulnyi, A.I. Kuklin, V.V. Novikov, A.V. Shibaev, O.E. Philippova, Transformations of wormlike surfactant micelles induced by a water-soluble monomer, J. Colloid Interface Sci. 602 (2021) 590–601, https://doi.org/10.1016/j.jcis.2021.05.062.
[45] S.R. Raghavan, G. Fritz, E.W. Kaler, Wormlike micelles formed by synergistic self-assembly in mixtures of anionic and cationic surfactants, Langmuir 18 (10) (2002) 3797–3803, https://doi.org/10.1021/la0115583.
[46] A.L. Kwiatkowski, V.S. Molchanov, H. Sharma, A.I. Kuklin, E.E. Dormidontova, O.E. Philippova, Growth of wormlike micelles of surfactant induced by embedded polymer: Role of polymer chain length, Soft Matter 14 (23) (2018) 4792–4804, https://doi.org/10.1039/c8sm00776d.
[47] B. Lindman, A. Khan, E. Marques, M.G. da Miguel, L. Piculell, K. Thalberg, Phase behavior of polymer-surfactant systems in relation to polymer-polymer and surfactant-surfactant mixtures, Pure Appl. Chem. 65 (1993) 953–958, https://doi.org/10.1351/pac199365050953.
[48] L.V. Angelova, P. Terech, I. Natali, L. Dei, E. Carretti, R.G. Weiss, Cosolvent gel-like materials from partially hydrolyzed poly(vinyl acetate)s and borax, Langmuir 27 (18) (2011) 11671–11682, https://doi.org/10.1021/la202179e.
[49] E.V. Korchagina, O.E. Philippova, Effects of hydrophobic substituents and salt on core–shell aggregates of hydrophobically modified chitosan: Light scattering study, Langmuir 28 (20) (2012) 7880–7888, https://doi.org/10.1021/la3013409.
[50] E. Pezron, L. Leibler, F. Lafuma, Complex formation in polymer-ion solutions. 2. Polyelectrolyte effects, Macromolecules 22 (6) (1989) 2656–2662, https://doi.org/10.1021/ma00196a021.
[51] J.M. Maerker, S.W. Sinton, Rheology resulting from shear-induced structure in associating polymer solutions, J. Rheol. 30 (1) (1986) 77–99, https://doi.org/10.1122/1.549898.
[52] S.W. Sinton, Complexation chemistry of sodium borate with poly(vinyl alcohol) and small diols: a boron-11 NMR study, Macromolecules 20 (10) (1987) 2430–2441, https://doi.org/10.1021/ma00176a018.
[53] H. Kurokawa, M. Shibayama, T. Ishimaru, S. Nomura, W. Wu, Phase behaviour and sol-gel transition of poly (vinyl alcohol)-borate complex in aqueous solution, Polymer 33 (10) (1992) 2182–2188, https://doi.org/10.1016/0032-3861(92)90886-2.
[54] C. Sommer, J.S. Pedersen, S.U. Egelhaaf, L. Cannavacciuolo, J. Kohlbrecher, P. Schurtenberger, Wormlike micelles as "equilibrium polyelectrolytes": Light and neutron scattering experiments, Langmuir 18 (2002) 2495–2505, https://doi.org/10.1021/la010214+.
[55] P. Schurtenberger, G. Jerke, C. Cavaco, J.S. Pedersen, Cross-section structure of cylindrical and polymer-like micelles from small-angle scattering data. 2. Experimental results, Langmuir 12 (10) (1996) 2433–2440, https://doi.org/10.1021/la9507444.
[56] R. Gamez-Corrales, J.-F. Berret, L.M. Walker, J. Oberdisse, Shear-thickening dilute surfactant solutions: Equilibrium structure as studied by small-angle neutron scattering, Langmuir 15 (20) (1999) 6755–6763, https://doi.org/10.1021/la990187b.
[57] A. Stradner, H. Sedgwick, F. Cardinaux, W.C.K. Poon, S.U. Egelhaaf, P. Schurtenberger, Equilibrium cluster formation in concentrated protein solutions and colloid, Nature 432 (2004) 492–495, https://doi.org/10.1038/nature03109.
[58] A. Shibaev, M. Gervais, I. Iliopoulos, O. Matsarskaia, G. Miquelard-Garnier, O. Philippova, S. Roland, C. Sollogoub. Microphase separation in double networks comprised of polymer and micellar chains. (2021) Institute Laue-Langevin (ILL), https://doi.org/10.5291/ILL-DATA.9-11-2009
[59] G.D. Wignall, R.G. Alamo, J.D. Londono, L. Mandelkern, F.C. Stehling, Small-angle neutron scattering investigations of liquid-liquid phase separation in heterogeneous linear low-density polyethylene, Macromolecules 29 (16) (1996) 5332–5335, https://doi.org/10.1021/ma960050h.
[60] M.E. Helgeson, Y.X. Gao, S.E. Moran, J.K. Lee, M. Godfrin, A. Tripathi, A. Bose, P.S. Doyle, Homogeneous percolation versus arrested phase separation in attractively-driven nanoemulsion colloidal gels, Soft Matter 10 (2014) 3122–3133, https://doi.org/10.1039/C3SM52951G.
[61] Y.Y. Xi, R.S. Lankone, L.P. Sung, Y. Liu, Tunable thermo-reversible bicontinuous nanoparticle gel driven by the binary solvent segregation, Nat. Comm. 12 (2021) 910, https://doi.org/10.1038/s41467-020-20701-3.
[62] Y. Xi, J.B. Leão, Q. Ye, R.S. Lankone, L.-P. Sung, Y. Liu, Controlling bicontinuous structures through a solvent segregation-driven gel, Langmuir 37 (6) (2021) 2170–2178, https://doi.org/10.1021/acs.langmuir.0c0347210.1021/acs.langmuir.0c03472.s001.
[63] A.R. Khokhlov, E.E. Dormidontova, Self-organization in ion-containing polymer systems, Physics-Uspekhi 40 (2) (1997) 109–124, https://doi.org/10.1070/PU1997v040n02ABEH000191.
[64] I.A. Nyrkova, A.R. Khokhlov, M. Doi, Microdomain structures in polyelectrolyte systems: Calculation of the phase diagrams by direct minimization of the free energy, Macromolecules 27 (15) (1994) 4220–4230, https://doi.org/10.1021/ma00093a025.
[65] A.M. Rumyantsev, J.J. de Pablo, Microphase separation in polyelectrolyte blends: Weak segregation theory and relation to nuclear "Pasta", Macromolecules 53 (4) (2020) 1281–1292, https://doi.org/10.1021/acs.macromol.9b02466.
[66] D.J. Grzetic, K.T. Delaney, G.H. Fredrickson, Electrostatic manipulation of phase behavior in immiscible charged polymer blends, Macromolecules 54 (6) (2021) 2604–2616, https://doi.org/10.1021/acs.macromol.1c00095.
[67] O.E. Philippova, A.S. Andreeva, A.R. Khokhlov, A.K. Islamov, A.I. Kuklin, V.I. Gordeliy, Charge-induced microphase separation in polyelectrolyte hydrogels with associating hydrophobic side chains: Small-angle neutron scattering study, Langmuir 19 (2003) 7240–7248, https://doi.org/10.1021/la034552h.
[68] A.S. Andreeva, O.E. Philippova, A.R. Khokhlov, A.K. Islamov, A.I. Kuklin, Effect of mobility of charged units on the microphase separation in amphiphilic polyelectrolyte hydrogels, Langmuir 21 (2005) 1216–1222, https://doi.org/10.1021/la0478999.
[69] E.Y. Kozhunova, V.Y. Rudyak, X. Li, M. Shibayama, G.S. Peters, O.V. Vyshivannaya, I.R. Nasimova, A.V. Chertovich, Microphase separation of stimuli-responsive interpenetrating network microgels investigated by scattering methods, J. Colloid Interface Sci. 597 (2021) 297–305, https://doi.org/10.1016/j.jcis.2021.03.178.
[70] M. Shibayama, F. Ikkai, S. Nomura, Complexation of poly(vinyl alcohol)-Congo Red aqueous solutions. 2. SANS and SAXS studies on sol-gel transition, Macromolecules 27 (22) (1994) 6383–6388, https://doi.org/10.1021/ma00100a023.
[71] A. Klymenko, T. Nicolai, L. Benyahia, C. Chassenieux, O. Colombani, E. Nicol, Multiresponsive hydrogels formed by interpenetrated self-assembled polymer networks, Macromolecules 47 (23) (2014) 8386–8393, https://doi.org/10.1021/ma501990r.
[72] M. Bellour, A. Knaebel, J.P. Munch, S.J. Candau, Scattering properties of salt-free wormlike micellar solutions, Eur. Phys. J. E 3 (2000) 111–121, https://doi.org/10.1007/s101890070024.
[73] K. Morishima, S. Sugawara, T. Yoshimura, M. Shibayama, Structure and rheology of wormlike micelles formed by fluorocarbon-hydrocarbon-type hybrid gemini surfactant in aqueous solution, Langmuir 33 (24) (2017) 6084–

6091, https://doi.org/10.1021/acs.langmuir.7b0090210.1021/acs.langmuir.7b00902.s001.
[74] L. Ziserman, L. Abezgauz, O. Ramon, S.R. Raghavan, D. Danino, Origins of the viscosity peak in wormlike micellar solutions. 1. Mixed catanionic surfactants. A cryo-transmission electron microscopy study, Langmuir 25 (18) (2009) 10483–10489, https://doi.org/10.1021/la901189k.
[75] Y. Han, Y. Feng, H. Sun, Z. Li, Y. Han, H. Wang, Wormlike micelles formed by sodium erucate in the presence of a tetraalkylammonium hydrotrope, J. Phys. Chem. B 115 (21) (2011) 6893–6902, https://doi.org/10.1021/jp2004634.
[76] D.P. Acharya, H. Kunieda, Wormlike micelles in mixed surfactant solutions, Adv. Colloid Interface Sci. 123–126 (2006) 401–413, https://doi.org/10.1016/j.cis.2006.05.024.
[77] R.H. Colby, Structure and linear viscoelasticity of flexible polymer solutions: Comparison of polyelectrolyte and neutral polymer solutions, Rheol. Acta 49 (5) (2010) 425–442, https://doi.org/10.1007/s00397-009-0413-5.
[78] P.J. Flory, J. Rehner, Statistical mechanics of cross-linked polymer networks I. Rubberlike elasticity, J. Chem. Phys. 11 (11) (1943) 512–520, https://doi.org/10.1063/1.1723791.
[79] A.Yu. Grosberg, A.R. Khokhlov, Giant Macromolecules: Here, There, and Everywhere. . .; Academic Press: San Diego, London, 1997.
[80] O.E. Philippova, A.R. Khokhlov. Polymer gels. In Polymer Science: A Comprehensive Reference, v. 1, pp. 339–366. Elsevier B.V USA, 2012.
[81] S. Roland, G. Miquelard-Garnier, A.V. Shibaev, A.L. Aleshina, A. Chennevière, O. Matsarskaia, C. Sollogoub, O.E. Philippova, I. Iliopoulos, Dual transient networks of polymer and micellar chains: Structure and viscoelastic synergy, Polymers 13 (23) (2021), https://doi.org/10.3390/polym13234255 4255.